


Materials for optical, magnetic and electronic devices

Accepted Manuscript

Volume 6
Number 5
7 February 2018
Pages 991-1265

Journal of Materials Chemistry C

Materials for optical, magnetic and electronic devices
rsc.li/materials-c



ISSN 2050-7526

PAPER
Hongyan Li, Mingyong, Yong-Ho Choe et al.
A redox gas sensor platform: linear device assemblies of
single-walled carbon nanotubes (SWCNTs) in a multi-layered
nanometric electrode systems (NLEES)

**ROYAL SOCIETY
OF CHEMISTRY**

Accepted Manuscripts are published online shortly after acceptance, before technical editing, formatting and proof reading. Using this free service, authors can make their results available to the community, in citable form, before we publish the edited article. We will replace this Accepted Manuscript with the edited and formatted Advance Article as soon as it is available.

You can find more information about Accepted Manuscripts in the [Information for Authors](#).

Please note that technical editing may introduce minor changes to the text and/or graphics, which may alter content. The journal's standard [Terms & Conditions](#) and the [Ethical guidelines](#) still apply. In no event shall the Royal Society of Chemistry be held responsible for any errors or omissions in this Accepted Manuscript or any consequences arising from the use of any information it contains.

Advances in modification of contradictory relationship: Simultaneously realizing large piezoelectricity and high Curie temperature in potassium sodium niobate based ferroelectrics

Jian Ma¹, Juan Wu¹, Bo Wu^{1, 2*} and Wenjuan Wu²

¹Sichuan province key laboratory of information materials, Southwest Minzu University, Chengdu 610041, P. R. China

²Sichuan Province Key Laboratory of Information Materials and Devices Application, Chengdu University of Information Technology, Chengdu 610225, P. R. China

*Corresponding author. Email: wubo7788@126.com (B. Wu.)

Abstract:

For potassium sodium niobate (KNN) based ferroelectrics, a critical contradictory relationship exists where higher piezoelectricity are often achieved at the cost of their Curie temperature, and severely restricts the practical process. How to resolve this contradiction is one of the urgent concerns in high-temperature piezoelectric applications. Here, a new material system of $0.965\text{K}_{0.54}\text{Na}_{0.46}\text{Nb}_{1-x}\text{Sb}_x\text{O}_3-0.03\text{Bi}_{0.5}\text{Na}_{0.5}\text{ZrO}_3-0.005\text{BiFeO}_3$ (KNNS_x-BNZ-BF, $0 \leq x \leq 0.03$) has been obtained by the compositional selection. A considerable progress on simultaneously realizing large d_{33} (~505 pC/N) and high T_C (~285 °C) is made in this ferroelectric, which is superior to the previously reported KNN-based ferroelectrics to date. In addition, good temperature-independent strain properties are also attained in this material due to high T_C values. Therefore, such a KNN-based system may promote the practical process of lead-free materials in high temperature fields.

Keywords: KNN; Piezoelectricity; Curie temperature

1. Introduction

View Article Online
DOI: 10.1039/D0TC01888K

As an indispensable part in electronic devices, piezoelectric materials have been paid extensive attentions due to their exceptional abilities to converting electrical energy into mechanical energy and vice versa. Lead zirconate titanate (PZT)-based ceramics have dominated current market of piezoelectric devices since 1950s on account of their high electric properties.¹ Although piezoelectric devices have the wide range of applications in the internet of things such as geothermal well-drilling tools and robot brakes, there is an increasing demand for materials with higher operation temperature (≥ 200 °C) in space exploration, electric aircraft, automobile engine, etc.²⁻³ However, traditional commercial PZT-based ceramics can hardly meet the above requirements.^{1,3} In addition, many countries are increasingly concerned about environmental risk and human health problem due to the toxicity of lead. Hence, it has to be urgent to develop lead-free material with good electric properties and high Curie temperature.⁴⁻¹⁰

Until now, several promising candidates of lead-free materials have been widely investigated, such as BaTiO₃ (BT)-based, Bi_{0.5}Na_{0.5}TiO₃ (BNT)-based, BiFeO₃ (BF)-based, and K_{0.5}Na_{0.5}NbO₃ (KNN)-based ceramics.¹¹⁻¹⁸ Generally, the BT-based ceramics have high piezoelectric properties but low Curie temperatures.^{9, 19-20} On the contrary, the BNT-based and BF-based ceramics usually have high Curie temperature but low piezoelectric properties.²¹⁻²² Although the KNN-based ceramics with relatively good comprehensive performance so far have been regarded as one of the most promising lead-free candidates, it still cannot be used in elevated temperature fields.⁴ To further analyze the relationship between piezoelectric properties (d_{33}) and Curie temperature (T_C) in piezoelectric materials, the d_{33} as well as T_C of several representative lead-free candidates and PZT-based ceramics are plotted in Fig.1.^{4, 11-14,}

18-23 Four regions (I: Low d_{33} and T_C ; II: High d_{33} and low T_C ; III: Low d_{33} and high T_C ; IV: High d_{33} and T_C) can be easily found in Fig.1 (a). The undoped-BT ceramics belong to the region I,⁹ the BT-based ceramics doped with Ca, Sr, Zr, Hf, and Sn locate at region II,^{9, 19-20} and the region III are comprised of BNT-based and BF-based ceramics.²¹⁻²² The KNN-based and PZT-based ceramics can occupy the region I to IV. Although they only hold in the left bottom of region IV, there is still possibility for the improvement of d_{33} and T_C .^{4, 11-14, 18, 23} Based on the above discussion, the critical contradictory relationship between d_{33} and T_C seriously restricts the piezoelectric ceramics in high temperature applications. It is urgent to make the development tendency of lead-free materials from region I, II and III to IV, as shown in Fig.1(b), expecting to solve the fundamental contradictions which arise between d_{33} and T_C , and further satisfy the rising demands for materials with higher operation temperature.

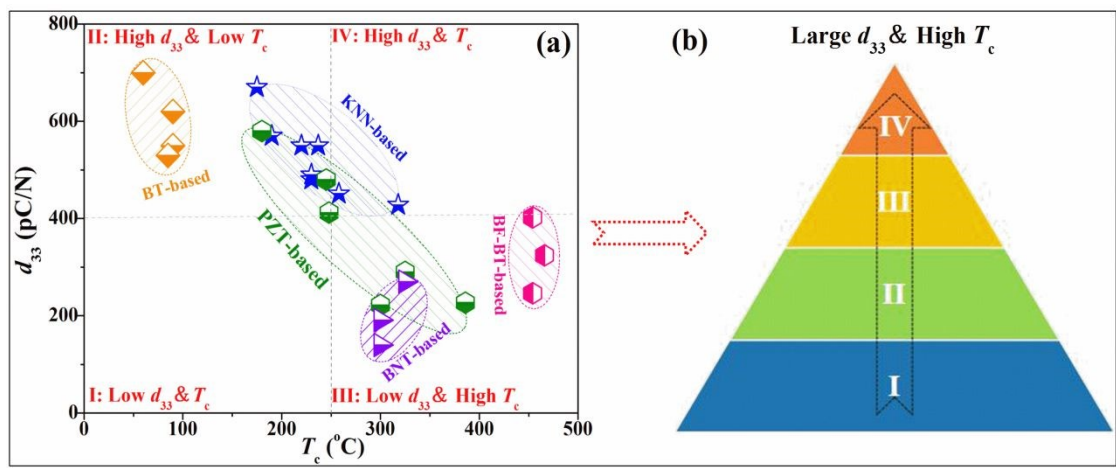


Fig.1: (a) d_{33} vs T_C of KNN-^{4, 11-14, 18} BT-^{9, 19-20} BNT-²¹ BF-²² and PZT-based materials;^{1, 11, 23} (b) schematic of recent development tendency of lead-free materials.

Among these lead-free piezoelectric ceramics, KNN-based ceramics have been regarded as one of the most promising lead free candidates to obtain both high d_{33} and

T_C . The rapid development of KNN-based ceramics by phase engineering strategy has been witnessed in recent years, which can largely improve the piezoelectric properties.^{4, 9-18, 26-28} Especially, shifting the phase transition temperatures [*e.g.*, rhombohedral-orthorhombic (T_{R-O}), orthorhombic-tetragonal (T_{O-T})] to room temperature simultaneously through chemical modifications is by far the most effective way to obtain higher piezoelectric properties ($d_{33} \geq 400$ pC/N).^{4, 9-18} Unfortunately, the higher d_{33} is often achieved at the cost of their T_C values. Such a situation can hardly satisfy the practical demand, which requires not only the high performances but also the high stability in response to ambient changes, especially the temperature environment.

The recent publications reveal that a high piezoelectric property can be easily obtained in the KNN-based material systems with codoping Sb and $\text{Bi}_{0.5}\text{M}_{0.5}\text{NO}_3$ (M: Na, K, Li, Ag; N: Zr, Hf, Sn), indicating that Sb and $\text{Bi}_{0.5}\text{M}_{0.5}\text{NO}_3$ play an important role in enhancing piezoelectric property.^{4, 24} In order to achieve the balance development of d_{33} and T_C , the systematic research on Sb should be carried out. It is reported that BiFeO_3 (BF) shows significantly high efficiency on shifting T_{R-O} and T_{O-T} to the vicinity of room temperature without decreasing T_C significantly.¹⁴ Therefore, the addition of BF can decrease the amount of Sb when constructing multiphase boundary and is beneficial to maintain a high T_C .¹⁴ Here, a new material system of $0.965\text{K}_{0.54}\text{Na}_{0.46}\text{Nb}_{1-x}\text{Sb}_x\text{O}_3-0.03\text{Bi}_{0.5}\text{Na}_{0.5}\text{ZrO}_3-0.005\text{BiFeO}_3$ ($\text{KNNS}_x\text{-BNZ-BF}$, $0 \leq x \leq 0.03$) with high d_{33} (~ 505 pC/N) and T_C (~ 285 °C) has designed, aiming to solve the fundamental contradictions between piezoelectric property and Curie temperature to satisfy the

rising demand for materials with higher operation temperature. Such an outstanding comprehensive property is superior to the previously reported lead-free materials, which has really achieved the balanced development of piezoelectricity and Curie temperature by composition modification in KNN-based ceramics, promoting the practical process of lead-free materials in high temperature fields. In addition, the physical mechanisms of the related phenomenon are clearly illuminated.

2. Experimental section

0.965K_{0.54}Na_{0.46}Nb_{1-x}Sb_xO₃-0.03Bi_{0.5}Na_{0.5}ZrO₃-0.005BiFeO₃ (KNNS_x-BNZ-BF, 0 ≤ *x* ≤ 0.03) lead-free piezoelectric ceramics were prepared by the conventional solid-state reaction process. Raw materials [Na₂CO₃ (99.8%), K₂CO₃ (99%), Nb₂O₅ (99.5%), Sb₂O₃ (99%), ZrO₂ (99%), Bi₂O₃ (99%), and Fe₂O₃ (99%)] were weighed according to above chemical formula, and then milled with ZrO₂ balls for 24 hours using alcohol as the dispersion medium in a plastic jar. The powder milled again with ZrO₂ balls for 8 hours after calcining at 850 °C for 6 hours. The calcined powders were mixed with a binder of 8 wt% polyvinyl alcohol (PVA) and pressed into the pellets with 10 mm diameter and 1 mm thickness under a pressure of 10 MPa. The PVA was burnt off afterwards. All disk samples were sintered at 1070–1085 °C for 3 h in air. All the samples were poled in a silicone oil bath at room temperature under a DC field of 3.0 kV/mm for 30 min.

X-ray diffraction meter with a CuKα radiation (DX-2700, Dandong, China) was used to identify the phase structure of the sintered cylindrical pellets. Their microstructure was measured by a field-emission scanning electron microscope (FE-SEM) (JSM-7500, Japan). The capacitance and dissipation factors of the sintered samples were measured

using an *LCR* analyzer (HP 4980, Agilent, U.S.A.) with varied temperatures between 100~200 °C and from room temperature to 450 °C. The *P-E* loops, *S-E* curves of the samples were investigated by the ferroelectric tester (aixACCT, TF Analyzer 2000E, Germany), and the PFM observations were conducted on a commercial atomic force microscope (MFP-3D origin+, Asylum Research, Goleta, CA, USA) with a conductive Pt-Ir-coated cantilever (NanoWorld EFM, force constant 2.8 N/m, resonance frequency 75 kHz).

3. Results and Discussion

To identify the phase structure evolution of $\text{KNNS}_x\text{-BNZ-BF}$ ceramics, the XRD patterns, ϵ_r -*T* curves, and Rietveld refinement XRD patterns are presented in Fig. 2. Fig. 2(a) shows XRD patterns of $\text{KNNS}_x\text{-BNZ-BF}$ ceramics, and the pure ABO_3 perovskite structure is observed in all ceramics, suggesting that the stable perovskite solid solution has been formed among the KNNS, BNZ, and BF. The ϵ_r -*T* (-100~200 °C) curves only present one dielectric peak in the measured temperature, indicating

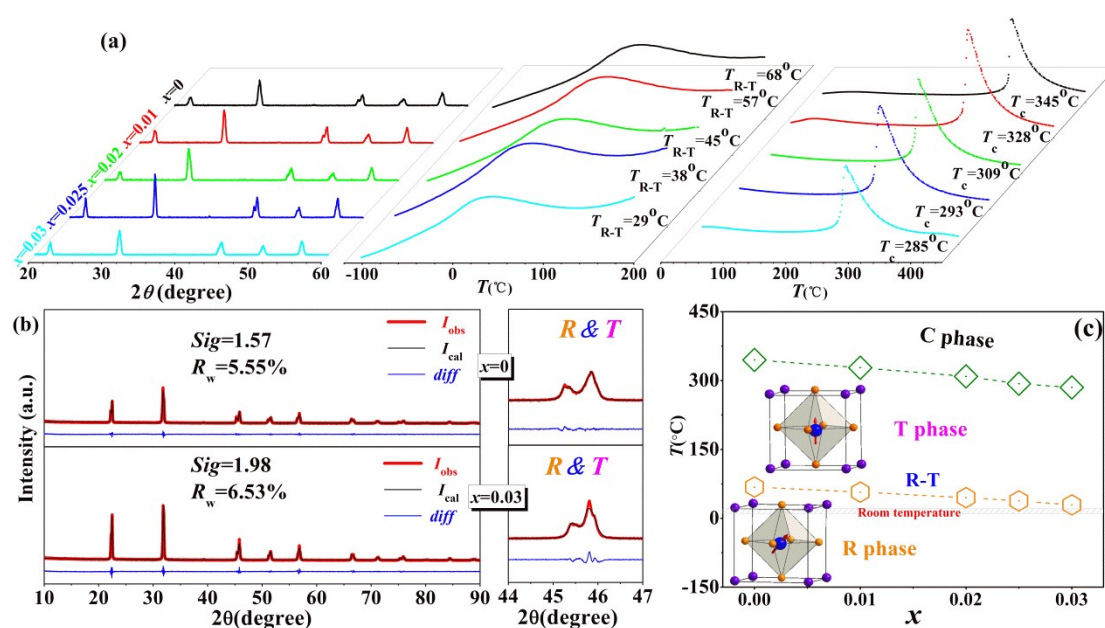


Fig.2: (a) XRD patterns in the 2θ range of 20–60° and ϵ_r -*T* (-100~200 °C; 30~450 °C)

curves of $\text{KNNS}_x\text{-BNZ-BF}$ ceramics; (b) Rietveld refinement on XRD patterns in the 2θ range of $20\text{--}90^\circ$ for $\text{KNNS}_x\text{-BNZ-BF}$ ceramics with $x=0, 0.03$; (c) Phase diagrams of $\text{KNNS}_x\text{-BNZ-BF}$ ceramics.

that all samples show R-T phase boundary at room temperature. The $\epsilon_r\text{--}T$ ($30\text{--}450^\circ\text{C}$) curves of the ceramics with $0 \leq x \leq 0.01$ have two obvious dielectric peaks, which is relevant to the R-T phase transition temperature ($T_{\text{R-T}}$) at low temperature side and Curie temperature (T_{C}) at high temperature side. The $\epsilon_r\text{--}T$ ($30\text{--}450^\circ\text{C}$) curves of the ceramics with $0.02 \leq x \leq 0.03$ only show one obvious dielectric peak corresponding to the T_{C} . Rietveld refinement XRD patterns is carried out to further identity the phase structure of ceramics with $x=0, 0.03$ [Fig. 2(b)], which can reflect the crystal symmetry of ceramics.²⁵ The results is highly consistent with the experimental XRD patterns, and a series of low Sig (≤ 1.98) and R_{w} ($\leq 6.53\%$) values are presented in calculated data, reconfirming the R-T phase boundary in $\text{KNNS}_x\text{-BNZ-BF}$ ceramics at $x=0, 0.03$ at room temperature. The corresponding refined parameters of ceramics are listed in the Table S1, such as space group, lattice parameters, etc. In addition, $\text{KNNS}_x\text{-BNZ-BF}$ ceramics' phase diagram is plotted in Fig. 2(c). The T_{C} ($\sim 345^\circ\text{C} \rightarrow 285^\circ\text{C}$) and $T_{\text{R-T}}$ ($\sim 68^\circ\text{C} \rightarrow 29^\circ\text{C}$) values monotony decrease with increasing Sb, as shown in Fig. 2(c). It is noticeable that a relative high T_{C} ($\geq 285^\circ\text{C}$) is obtained in $\text{KNNS}_x\text{-BNZ-BF}$ ceramics. As we know, Sb plays an important role on enhancing piezoelectric property in KNN-based piezoelectrics by the formation of multiphase boundaries, while T_{C} is also sacrificed a lot simultaneously.^{4, 24} BF exhibits significantly high efficiency on shifting $T_{\text{R-O}}$ and $T_{\text{O-T}}$ to the vicinity of room temperature without a significant decrease in T_{C} .¹⁴ Therefore, introducing appropriate amount of BF to this ferroelectric can reduce the Sb content, which is beneficial to the balance development of d_{33} and T_{C} .

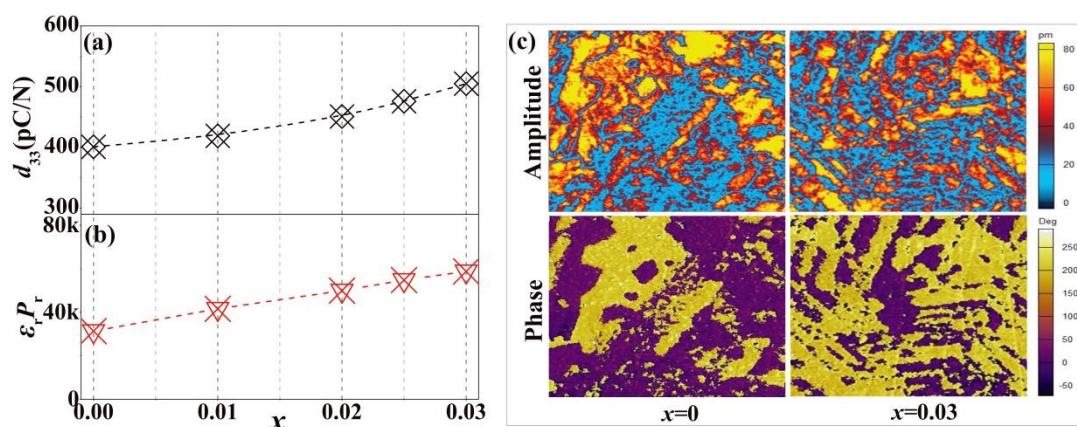


Fig.3: (a) d_{33} and (b) $\epsilon_r P_r$ of $\text{KNNS}_x\text{-BNZ-BF}$ ceramics. (c) Vertical piezoelectric force microscopy (V-PFM) results showing amplitude and phase images for $\text{KNNS}_x\text{-BNZ-BF}$ ceramics with $x=0, 0.03$.

The piezoelectric, dielectric, ferroelectric, and strain properties of $\text{KNNS}_x\text{-BNZ-BF}$ ceramics are plotted in Fig.3 and Figs.S1-S2. Here, we just focus on the variation of piezoelectric constant (d_{33}) as a function of Sb content, as shown in Fig. 3(a). The d_{33} linearly increases with increasing Sb^{5+} due to the phase boundary closing to room temperature, and an optimal piezoelectric performance of $d_{33} \sim 505$ pC/N is obtained in the ceramics with $x=0.03$, which is superior or compared to that of PZT-based ceramics. Such an excellent piezoelectric property can be explained by the following reasons. Firstly, the R-T phase boundary with low polarization anisotropy and weak energy barriers can greatly improve piezoelectricity.^{14, 18} Secondly, the good dielectric and ferroelectric properties also play an important role in enhancing piezoelectric property. Generally, the formula of $d_{33} \sim \alpha \epsilon_r P_r$ can be well evaluated the relationship of dielectric, ferroelectric and piezoelectric properties.^{4, 14, 18} Fig. 3(b) plots the $\epsilon_r P_r$ against Sb^{5+} , and

the ϵ_r and P_r are presented in Figs.S1-S2. The $\epsilon_r P_r$ monotonically increase with the increase of Sb^{5+} , and is well matched with the variation of d_{33} values, which demonstrates the enhancement of d_{33} benefits from the improvement of ϵ_r and P_r . Thirdly, the domain structures significantly contribute to piezoelectric properties in piezoelectric materials. To illustrate the strong relevance between d_{33} and domain structure, the vertical piezoresponse force microscopy (V-PFM) is carried out to figure out the domain configuration and response, as is shown in Fig.3(c). The amplitude and phase images are consistent with each other, presenting complicated domain patterns with micron-size or submicron-size domains in the ceramics with $x=0, 0.03$. For the ceramic at $x=0$, a series of inhomogeneous and block domains is clearly observed. The substantially irregular domains with widths of several hundred nanometers and small amount of block domains are obtained in the ceramic with $x=0.03$, resulting from the decreasing of domain wall energy near multiphase boundary regions. Several publications reported that the domains size is in the inverse proportional relationship to the piezoelectric property because small domains are more easily switched than the larger ones under the external electric field.^{12, 29-30} The high ratio of small domains in the ceramics with $x=0.03$ may account for the enhancement of piezoelectric property. Therefore, the excellent piezoelectric property in the samples with $x=0.03$ can be ascribed to the R-T phase boundary, the improvement of ϵ_r and P_r , and relatively small domains structure.

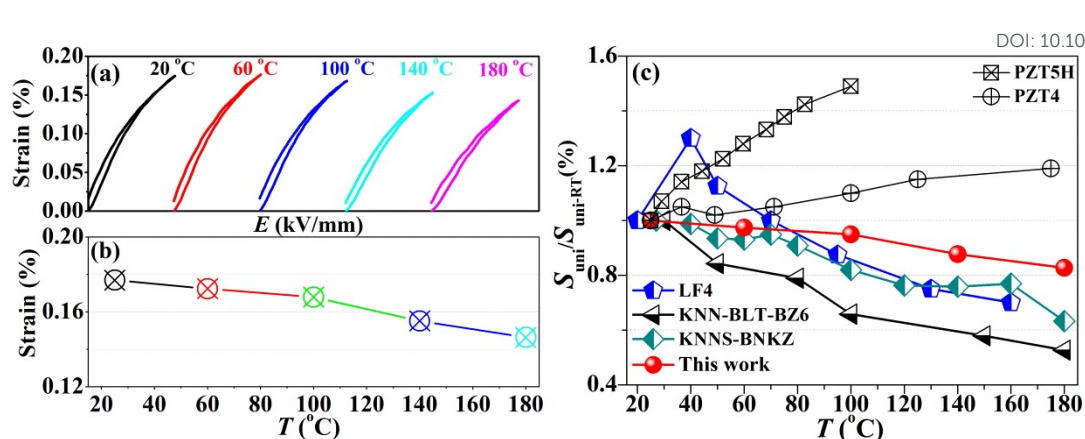


Fig.4: Temperature-dependent (a) unipolar strain and (b) S_{uni} for the ceramic with $x=0.03$. (c) Comparison of temperature-dependent normalized S_{uni} for typical KNN-based and PZT-based materials systems.

Because the extremely harsh working temperature environment has become one of the biggest challenges for the applications of KNN-based ceramics, it is necessary to make a systematic study for the temperature-dependent strain property. Typical unipolar strain curves of $x=0.03$ are obtained in the temperature range of 20-180 °C, and the unipolar strain S_{uni} slowly decreases with increasing temperature, as shown in Fig.4(a)-(b). Note that a high S_{uni} of ~0.146% is kept even at high temperature of 180 °C, which results from the high T_C (~285 °C) of the samples. The temperature-dependent strain (in terms of normalized strain value) of several representative KNN-based and PZT-based piezoceramics is also provided in Fig. 4(c) for comparison. An excellent temperature stability of S_{uni} is achieved in this work with fluctuating less than 17.6% in the investigated temperature range because of its high T_C , which is also superior or compare to other KNN-based or PZT-based materials.^{11, 13, 31-33}

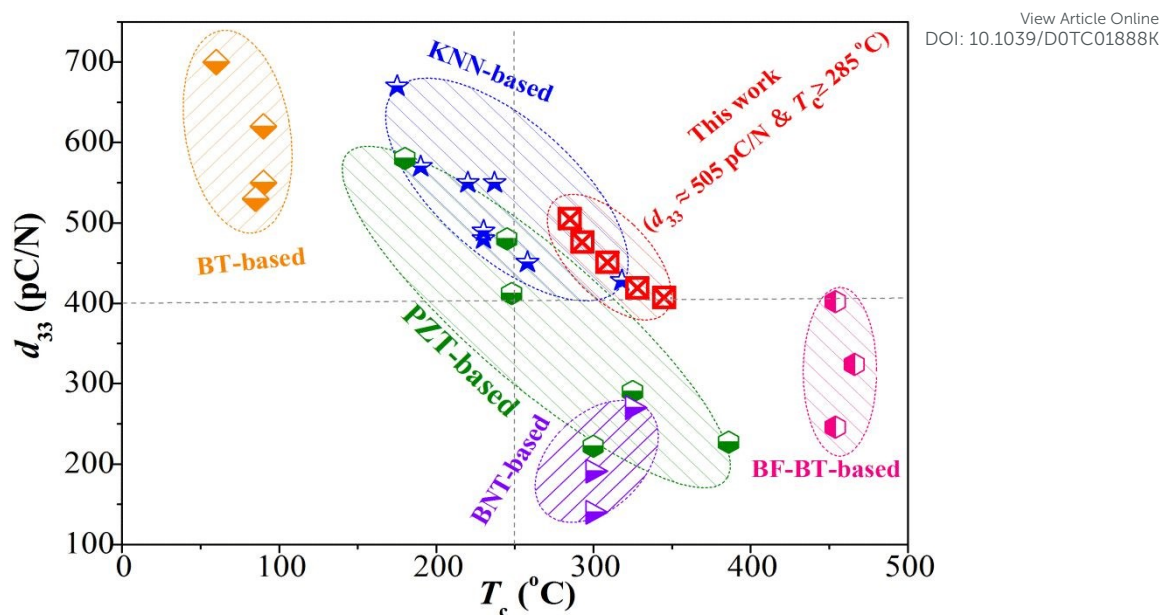


Fig.5: d_{33} vs T_c of KNN-,^{4,11-14,18} BT-,^{9,19-20} BNT-,²¹ BF-,²² and PZT-based materials.^{1,}

11, 23

An outstanding comprehensive property ($d_{33} \sim 505$ pC/N, and $T_c \sim 285$ °C) is indeed simultaneously realized in KNN-based ferroelectrics, as is shown in Fig.5, which is superior to the previously reported results in other KNN-based materials and some typical PZT-based ceramics. Such an excellent comprehensive property has achieved the balanced development of piezoelectricity and Curie temperature by composition modification in KNN-based ceramics, providing a paradigm for designing KNN-based ferroelectric with the large piezoelectricity in a wide working temperature range.

4. Conclusions

0.965K_{0.54}Na_{0.46}Nb_{1-x}Sb_xO₃-0.03Bi_{0.5}Na_{0.5}ZrO₃-0.005BiFeO₃ lead-free ceramics with high d_{33} (~ 505 pC/N) as well as T_c (~ 285 °C) were prepared by the normal sintering method, and the phase boundary, piezoelectric, ferroelectric, and strain properties were studied. Such an outstanding comprehensive property is superior to the previously

reported results in lead-free materials, which has achieved the balanced development of piezoelectricity and Curie temperature by composition modification in KNN-based ceramics. It may offer a paradigm for designing KNN-based ferroelectric with the large piezoelectricity in a wide working temperature range, promoting the practical process of lead-free materials in high temperature fields.

Notes

The authors declare no conflict of interest.

Acknowledgements

Authors gratefully acknowledge the supports of the National Science Foundations of China (NSFC Nos. 51702028 and 51702029), and the Electronic information engineering (Southwest Minzu University) key laboratory opening project of national civil affairs commission (Grant No. IM19002).

References

1. B. Jaffe, Piezoelectric ceramics, Elsevier, 2012.
2. S. Chen, X. L. Dong, C. L. Mao, and F. Cao, *J. Am. Ceram. Soc.*, 89, 3270–2 (2006).
3. F. Gao, R. Hong, and J. Liu, *J. Eur. Ceram. Soc.*, 29, 1687–93 (2009).
4. J. G. Wu, D. Q. Xiao, J. G. Zhu, *Chem. Rev.* 2015, 115, 2559.
5. C. H. Hong, H. P. Kim, B. Y. Choi, H. S. Han, J. S. Son, A. W. Chang, W. Jo, *J. Materiomics*, 2016, 2(1), 1–24.
6. J. Rödel, W. Jo, K. T. P. Seifert, E. M. Anton, T. Granzow, D. Damjanovic, *J. Am. Ceram. Soc.*, 2009, 92(6), 1153.
7. J. F. Li, K. Wang, F. Y. Zhu, L. Q. Cheng, F. Z. Yao, *J. Am. Ceram. Soc.*, 2013, 96(12), 3677.
8. J. Hao, W. Li, J. Zhai, H. Chen, *Mater. Sci. Eng., R*, 2019, 135, 1.
9. T. Zheng, J. Wu, D. Xiao, J. Zhu, *Prog. Mater. Sci.*, 2018, 98, 552.
10. J. Wu, D. Xiao, J. Zhu, *J. Mater. Sci: Mater. Electron.* 2015; 26: 9297.
11. Y. Saito, H. Takao, T. Tani, T. Nonoyama, K. Takatori, T. Homma, T. Nagaya, M.

Nakamura, *Nature*. 2004, 432, 84.

View Article Online
DOI: 10.1039/D0TC01888K

12. K. Xu, J. Li, X. Lv, J. Wu, X. Zhang, D. Xiao, J. Zhu, *Adv. Mater.* 2016, 28, 8519.
13. T. Zheng, H. Wu, Y. Yuan, X. Lv, Q. Li, T. Men, C. Zhao, D. Xiao, J. Wu, K. Wang, J. Li, Y. Gu, J. Zhu, S. Pennycook, *Energy. Environ. Sci.* 2017, 10, 528.
14. B. Wu, H. Wu, J. Wu, D. Xiao, J. Zhu, S. Pennycook, *J. Am. Chem. Soc.* 2016, 138, 15459.
15. X. Wang, J. Wu, D. Xiao, J. Zhu, X. Cheng, T. Zheng, B. Zhang, X. Lou, X. Wang, *J. Am. Chem. Soc.*, 2014, 136(7), 2905.
16. Q. Liu, Y. Zhang, J. Gao, Z. Zhou, H. Wang, K. Wang, X. Zhang, J. F. Li, *Energy. Environ. Sci.*, 2018, 11(12), 3531.
17. M. H. Zhang, K. Wang, Y. J. Du, G. Dai, W. Sun, G. Li, D. Hu, H. C. Thong, C. L. Zhao, X. Q. Xi, Z. X. Yue, J. F. Li, *J. Am. Chem. Soc.*, 2017, 139, 3889.
18. H. Tao, H. Wu, Y. Liu, Y. Zhang, J. Wu, F. Li, X. Lyu, C. Zhao, D. Xiao, J. Zhu, S. Pennycook, *J. Am. Chem. Soc.*, 2019, 141, 13987.
19. W. F. Liu, X. B. Ren, *Phys. Rev. Lett.*, 2009, 103(25), 257602.
20. C. Zhao, H. Wu, F. Li, Y. Cai, Y. Zhang, D. Song, J. Wu, X. Lyu, J. Yin, D. Xiao, J. Zhu, S. J. Pennycook, *J. Am. Chem. Soc.*, 2018, 140(45), 15252.
21. J. Yin, C. L. Zhao, Y. X. Zhang, J. G. Wu, *J. Am. Ceram. Soc.* 2017, 100, 5601.
22. M. H. Lee, D. J. Kim, J. S. Park, S. W. Kim, T. K. Song, M. H. Kim, W. J. Kim, D. Do, K. Jeong, *Adv. Mater.* 2015, 27, 6976.
23. M. W. Hooker, Technical Report No. NASA/CR-1998-208708.
24. J. Wu, H. Tao, Y. Yuan, X. Lv, X. Wang, X. Lou, *RSC Adv.*, 2015, 5, 14575.
25. J. Gao, D. Xue, Y. Wang, D. Wang, L. Zhang, H. Wu, S. Guo, H. Bao, C. Zhou, W. Liu, *Appl. Phys. Lett.* 2011, 99, 092901
26. Y. Yuan, J. Wu, T. Hong, X. Lv, X. Wang, and X. Lou, *J. Appl. Phys.*, 2015, 117, 084103.
27. B. Wu, J. Ma, W. J. Wu, M. Chen, *J. Mater. Chem. C*, 2020, 8, 2838.
28. W. J. Wu, J. Ma, B. Wu, Q. Gou, M. Chen, *J. Alloys Compd.*, 2020, 822, 153585.
29. J. Gao, Y. Hao, S. Ren, T. Kimoto, M. Fang, H. Li, Y. Wang, L. Zhong, S. Li, X. Ren, *J. Appl. Phys.* 2015, 117, 084106.
30. Y. Huan, X. H. Wang, Z. B. Shen, J. Y. Kim, H. H. Zhou, L. T. Li, *J. Am. Ceram.*

Soc. 2014, 97, 700.

View Article Online
DOI: 10.1039/D0TC01888K

31. R. Wang, K. Wang, F. Yao, J. F. Li, F. H. Schader, K. G. Webber, W. Jo, J. Rödel, J. Am. Chem. Soc., 2015, 98, 2177.

32. D. Wang, Y. Fotinich, G. P. Carman, J. Appl. Phys. 1998, 83, 5342.

33. K. Wang, F.-Z. Yao, W. Jo, D. Gobeljic, V. V. Shvartsman, D. C. Lupascu, J.-F. Li and J. Roedel, Adv. Funct. Mater., 2013, 23, 4079.

Table of contents entry

View Article Online
DOI: 10.1039/D0TC01888K

Modification of contradictory relationship between piezoelectricity and Curie temperature in potassium sodium niobate based piezoceramics

Jian Ma¹, Juan Wu¹, Bo Wu^{1, 2*} and Wenjuan Wu²

¹Sichuan province key laboratory of information materials, Southwest Minzu University, Chengdu 610041, P. R. China

²Sichuan Province Key Laboratory of Information Materials and Devices Application, Chengdu University of Information Technology, Chengdu 610225, P. R. China

*Corresponding author. Email: wubo7788@126.com (B. Wu.)

We decode the relationship of balanced development between piezoelectricity and Curie temperature, which would be promoted the practical process of in KNN-based ceramics in high temperature fields.

